Haploinsufficiency of kelch-like protein homolog 10 causes infertility in male mice

Wei Yan*†, Lang Ma*, Kathleen H. Burns*, and Martin M. Matzuk*‡§

Departments of *Pathology, ‡Molecular and Human Genetics, and §Molecular and Cellular Biology, Baylor College of Medicine, One Baylor Plaza, Houston, TX 77030

Edited by Ryuzo Yanagimachi, University of Hawaii, Honolulu, HI, and approved April 5, 2004 (received for review December 4, 2003)

We identified a testis-specific gene encoding a protein containing a BTB/POZ domain and six kelch repeats, which we named kelch homolog 10 (KLHL10). KLHL10 displays high evolutionary conservation in mammals, as evidenced by 98.7% amino acid identity between mouse and human KLHL10. KLHL10 is exclusively expressed in the cytoplasm of elongating and elongated spermatids (steps 9–16). We generated a *Klhl10* null allele in 129S6/SvEv mouse embryonic stem cells, and obtained 47 chimeras from six independent embryonic stem cell lines. Whereas low-percentage male chimeras only produce C57BL/6J offspring, high-percentage chimeric and heterozygous males were completely infertile because of disrupted spermiogenesis characterized by asynchronous spermatid maturation, degeneration of late spermatids, sloughing of postmeiotic germ cells from the seminiferous epithelium, and marked reduction in the numbers of late spermatids. Our data demonstrate that, like protamine-1 and -2, both alleles of *Klhl10* are required for male fertility and that haploinsufficiency caused by a mutation in one allele of *Klhl10* prevents genetic transmission of both mutant and WT alleles.

spermatogenesis | spermiogenesis | ubiquitination | knockout | *in silico* subtraction

Spermiogenesis is the process by which round spermatids differentiate into elongating and elongated spermatids. During this process, haploid male germ cells undergo dramatic morphological changes, and multiple cellular events unique to male germ cells take place, including acrosome formation, nuclear condensation and packaging, tail formation, reorganization of cytoplasm and organelles, and spermiation (1). A striking feature of spermiogenesis is the coordinated development of germ cells that not only synchronizes maturation of each individual germ-cell population, but also specifically associates different germ-cell populations within a specific tubule stage in mice (2). Given the complexity of cellular events during spermiogenesis, one would expect a multitude of elaborate regulatory processes at transcriptional, translational, and posttranslational levels. However, the molecular mechanisms responsible for these changes remain largely unknown. With gene-knockout technology, >30 proteins have been shown to play important roles during spermiogenesis (3). Targeted mutations of these genes result in disrupted spermiogenesis.

Of human male-infertility cases ≈75% are idiopathic and disruption of spermiogenesis is often seen in these patients (4–6). Additionally, haploid germ cells are good targets for male contraceptives for the following reasons: (*i*) haploid germ cells express numerous unique genes and many of them encode membrane proteins, enzymes, and signaling molecules (7); (*ii*) unlike spermatocytes or spermatogonia, whose anomalies often affect other germ-cell populations and result in "Sertoli cell-only" seminiferous epithelium, degeneration of haploid germ cells rarely impairs the entire spermatogenic process; and (*iii*) all genomic remodeling events are accomplished at the spermatocyte stage (2). Thus, targeting haploid germ cells might be specific and reversible and have minimal risks to genomic integrity.

In a search for genes expressed exclusively by male haploid germ cells, we identified a testis-specific gene encoding a protein containing a BTB/POZ domain and six kelch repeats, which we named kelch homolog 10 (KLHL10). Here, we report our initial efforts to characterize the physiological roles of KLHL10.

Materials and Methods

***In Silico* Subtraction and Genomic Database Mining.** Expressed sequence tags (49,064) from three libraries [Lib.6786 (round spermatids), Lib.2547 (adult testis), and Lib.2511 (adult testis)] were downloaded from the mouse Unigene database (www.ncbi.nlm.nih.gov/UniGene/clust.cgi?ORG=Mm) at the National Center for Biotechnology Information (www.ncbi.nlm.nih.gov). *In silico* subtraction and genomic database mining were performed as described (8).

RNA and Protein Analyses. RNA and protein analyses were performed as described (9).

Generation and Genotype Analysis of *Klhl10* Mutant Mice. A targeting vector for *Klhl10* was constructed containing *Pgk-HPRT* and *MC1-tk* (thymidine kinase) expression cassettes (see Fig. 3*A*). The linearized *Klhl10* targeting vector was electroporated into AB2.2 embryonic stem (ES) cells and targeted clones were selected and identified as described (10).

Histology. Testes and epididymides were dissected, fixed in Bouin's fixative, and embedded in paraffin. Sections (5 μm) were prepared and stained with hematoxylin and eosin as described (10). For high-power (magnification, ×1,000) histological analyses, semithin sections (2.0 μm) were cut from testis samples fixed with 5% glutaraldehyde in 0.05 M cacodylate buffer (pH 7.4) at 4°C overnight. The postfixation treatment, dehydration, embedding, and staining with 1% toluidine blue were performed as described (11).

Transillumination-Assisted Microdissection of Seminiferous Tubules. Mouse seminiferous tubules were staged and dissected based on their transillumination patterns under a stereomicroscope as described (12). The stages of dissected tubule segments were further confirmed by observing the morphology of developing spermatids and their associating spermatocytes by using phase-contrast microscopy as described (12). For Western blot analy-

This paper was submitted directly (Track II) to the PNAS office.

Abbreviations: KLHL10, kelch-like homolog 10; ES, embryonic stem; TUNEL, terminal deoxynucleotidyltransferase-mediated dUTP-biotin nick end labeling; HPC, high-percentage chimeric; LPC, low-percentage chimeric.

Data deposition: The sequences reported in this paper have been deposited in the GenBank database [accession nos. AY495337 (mouse *Klhl10* cDNA), AY495338 (rat *Klhl10* cDNA), and AY495339 (human *Klhl10* cDNA)].

†To whom correspondence should be sent at the present address: Department of Physiology and Cell Biology, University of Nevada School of Medicine, 1604 North Virginia Street, Reno, NV 89557.

PHYSIOLOGY

ses, seminiferous tubule segments were divided into four groups from stages II–VI, VII–VIII, IX–XI, and XII–I.

Terminal Deoxynucleotidyltransferase-Mediated dUTP-Biotin Nick End Labeling (TUNEL) Analysis. Paraformaldehyde (4%)-fixed testis sections were used for TUNEL analysis of apoptotic cells by ApoTag Plus peroxidase kit (Intergen, Purchase, NY), according to the manufacturer's instructions.

Sperm Genotyping. Sperm were collected from the testis and epididymis as described (13, 14). DNA purification and genotyping for a microsatellite in the D2Mit94 locus of mouse chromosome 2 was performed as described (15). A comprehensive description of the methods and materials is available in *Supporting Text,* which is published as supporting information on the PNAS web site.

Results and Discussion

***Klhl10* Is a Testis-Specific Gene Exclusively Expressed in Spermatids.** Using *in silico* subtraction, we identified a cDNA encoding a kelch repeat-containing protein from a round spermatid library (Lib.6786) in the UniGene collection at the National Center for Biotechnology Information. The Mouse Gene Nomenclature Committee at The Jackson Laboratory assigned our gene the name kelch homolog 10 (*Klhl10*). A total of 46 expressed sequence tags potentially encoding KLHL10 have been grouped into UniGene cluster Mm.34168. Forty-five of these expressed sequence tags are derived from testis, whereas only one (AA199573) is from a mouse thymus library. We examined the possible expression of *Klhl10* in the thymus by RT-PCR and detected no signal (data not shown), suggesting that this expressed sequence tag in the National Center for Biotechnology Information database is a spurious finding possibly due to contamination. To confirm our *in silico* findings, we performed Northern blot and RT-PCR analyses with RNA samples from multiple tissues of mice (Fig. 1*A*) and humans (Fig. 1*B*). *Klhl10* is exclusively expressed in the testis in both mice and humans. Northern blot analyses of developing testes (Fig. 1*C*) show that *Klhl10* mRNA is first detectable at postnatal day 18 [when round spermatids first appear (16)], and levels of *Klhl10* mRNA increase thereafter until adulthood, suggesting that *Klhl10* is expressed in spermatids. Consistent with these data, *in situ* hybridization analyses localize *Klhl10* mRNA (Fig. 1*D*) to spermatids at all maturation steps. The expression windows of *Klhl10* mRNA and protein (see below and Fig. 2*E*) during mouse spermiogenesis are summarized in Fig. 1*E*.

KLHL10 Belongs to a Large Kelch Repeat Protein Superfamily. By genomic database mining, we identified KLHL10 orthologs in rat and human, which show high evolutionary conservation (Fig. 2*A*). Humans and mice KLHL10 proteins differ by only 7 of 608 aa; rat and mouse only differ by one amino acid, suggesting that KLHL10 is highly conserved during evolution and has important roles in spermatid development. Examination of the primary structure of KLHL10 reveals that it belongs to a large kelch repeat-containing protein superfamily (17). KLHL10 is similar to a subgroup of this protein family, which contains an N-terminal BTB/POZ domain and a C-terminal six kelch motifs (17) (Fig. 2*B*). Recent studies show that BTB domain-containing proteins interact with Cullin 3 ubiquitin ligases through a conserved N-terminal domain and are substrate-specific adaptors of the BCR (BTB-Cul3-Roc1) E3 ubiquitin ligases (18–23). The C-terminal half of KLHL10 is composed of six kelch motifs initially identified in the *Drosophila melanogaster* kelch ORF1 protein (24). The kelch repeats are predicted to adopt a blade-like conformation and assemble in a β-propeller structure, similar to that of galactose oxidase (25). Besides mediation of ubiquitin transfer, they have been implicated in diverse cellular

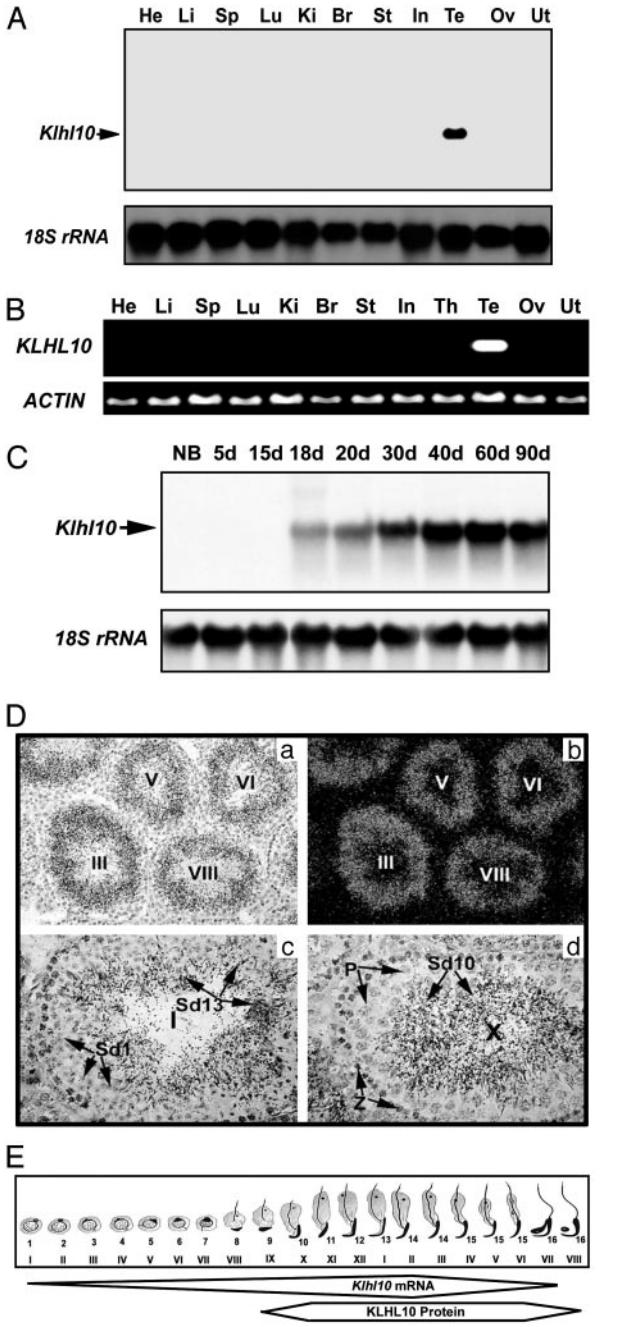

Fig. 1. Expression and localization of *Klhl10* mRNA in mouse and human tissues. (*A*) Northern blot analysis of *Klhl10* mRNA expression in mouse tissues including heart (He), liver (Li), spleen (Sp), lung (Lu), kidney (Ki), brain (Br), stomach (St), small intestine (In), testis (Te), ovary (Ov), and uterus (Ut). 18S rRNA was used as a loading control. (*B*) RT-PCR analysis of *KLHL10* expression in human tissues [(abbreviations are similar to *A*, except for thymus (Th)]. ACTIN was used as a loading control. (*C*) Northern blot analysis of *Klhl10* mRNA expression in mouse developing testes at ages of newborn (NB, ≈0.5 day) and 5–90 days (5–90d). 18S rRNA was used as a loading control. (*D*) Localization of *Klhl10* mRNA in the mouse testis by using *in situ* hybridization. Dark (*b*) and bright (*a*, *c*, and *d*) field images are shown. Lower magnification (*a* and *b*, ×100; *c* and *d*, ×400) images show that the signals are located in the luminal compartment, and higher magnification (*c* and *d*, ×400) images show that the signals are confined to spermatids at all maturation steps. (*E*) Schematic summary of the expression pattern of *Klhl10* mRNA and protein during spermiogenesis based on *C* and Fig. 2*E*. Frames represent the expression windows of *Klhl10* mRNA and protein, and the width of the frames represents expression levels. Arabic numbers represent the steps of spermatids, and Roman numerals indicate stages of the seminiferous epithelial cycle.

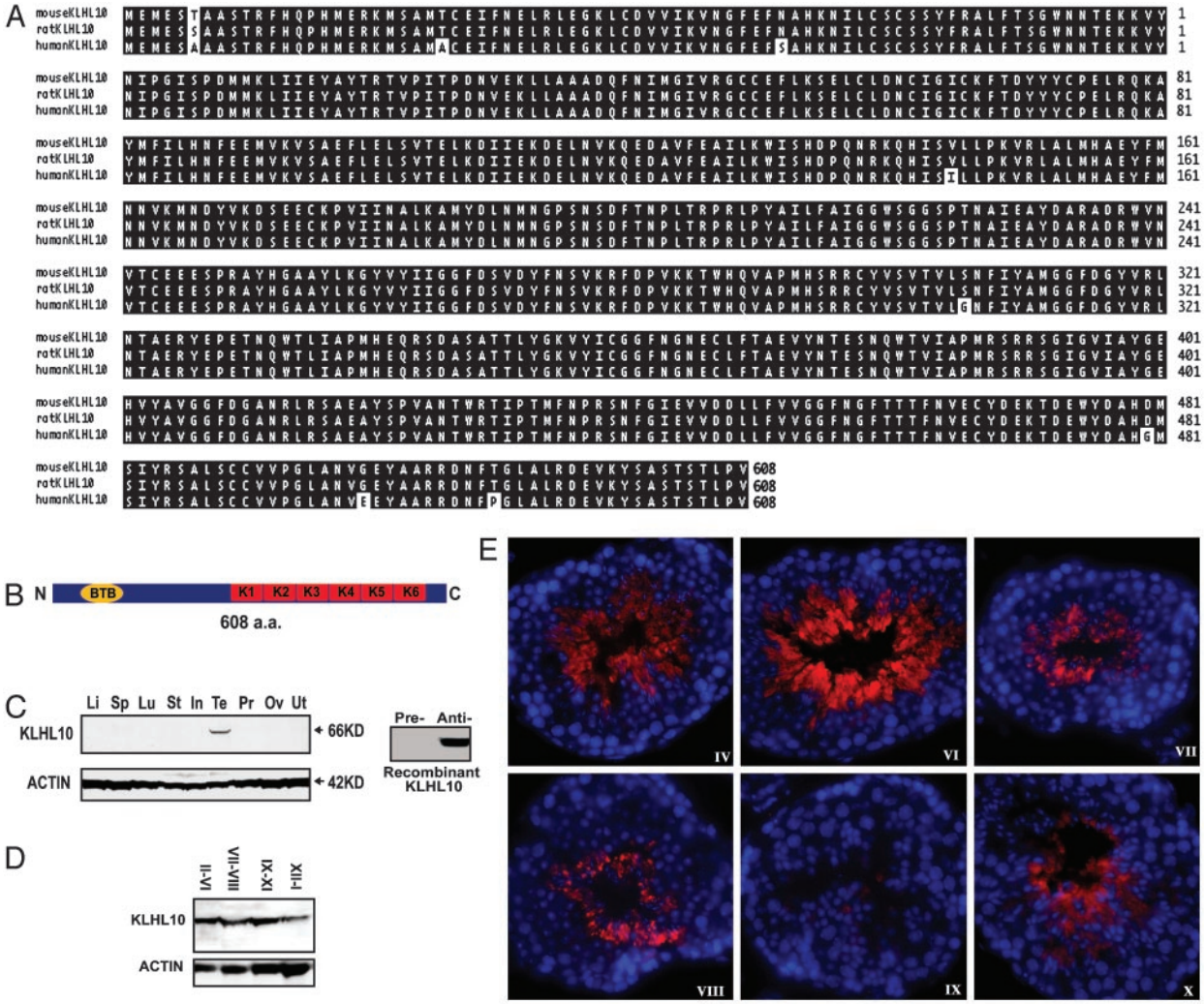

Fig. 2. Alignment, domain structure, and expression analyses of mouse KLHL10 and its orthologs. (*A*) Alignment analysis of mouse, rat, and human KLHL10. Identical residues are highlighted. (*B*) Domain structure of KLHL10. KLHL10 (608 aa) consists of an N-terminal BTB or POZ domain and six C-terminal kelch repeats. (*C*) Western blot analysis of KLHL10 in multiple mouse tissues (*Left*) including liver (Li), spleen (Sp), lung (Lu), stomach (St), small intestine (In), testis (Te), prostate (Pr), ovary (Ov), and uterus (Ut). ACTIN was used as a loading control. Unlike the KLHL10 antisera (Anti-), the preimmune serum (Pre-) does not react with KLHL10 recombinant protein (*Right*). (*D*) Western blot analysis of KLHL10 in four pooled, staged seminiferous tubules. Roman numerals represent stages of the seminiferous tubules. ACTIN was used as a loading control. (*E*) Immunofluorescent analysis of KLHL10 in the adult mouse testis. KLHL10 expression (red) is confined to the cytoplasm of elongating and elongated spermatids (steps 9–16). Blue represents 4′,6-diamidino-2-phenylindole staining of the nuclei of testicular cells, and stages are marked with Roman numerals.

processes, including actin cytoskeleton interaction [mayven (26), Kelch1 (27), and ENC1 (28)], regulation of cell morphology [Calcin (29)], and cytoplasmic sequestration of transcription factors [Keapl (30)]. Similarities in the domain structure among members of this subgroup suggest that KLHL10 may function as a cytoskeletal protein involved in spermatid architecture or as a component of E3 ubiquitin ligase complexes involved in ubiquitination pathways during spermiogenesis.

KLHL10 Is a Cytoplasmic Protein Expressed in Elongating and Elongated Spermatids. Western blot analyses on multiple tissues reveal that KLHL10 is exclusively expressed in the testis (Fig. 2*C*), which is consistent with our mRNA analyses (Fig. 1). Preimmune serum did not react with the recombinant KLHL10 protein (Fig. 2*C*), and detected no signal in the multiple-tissue Western blot analyses (data not show), indicating that our KLHL10 antibodies are the result of a specific immune response. Western blot analyses of four pooled stages of seminiferous tubules show that levels of KLHL10 display a stage-specific pattern with higher levels in stages II–VI and IX–XI, and lower levels in stages XII–I (Fig. 2 *C* and *D*). Immunofluorescent analysis localized KLHL10 to the cytoplasm of step 9–16 spermatids (Fig. 2*E*). KLHL10 displays a diffuse expression pattern within the cytoplasm of elongating and elongated spermatids. After spermiation, the majority of KLHL10 is retained in residual bodies (Fig. 2*E*, stage IX). *Klhl10* mRNA is expressed in steps 1–16 spermatids, whereas its protein is detectable in steps 9–16 spermatids. The delay between the onset of mRNA and protein expression of *Klhl10* suggests a posttranscriptional regulation, which is common to many spermatid-specific genes because transcription ceases after step 9 spermatids (31–36).

Because some members of the BTB/Kelch protein family function as cytoskeletal proteins through interactions with actins (17), we performed immunofluorescent colocalization analysis by using confocal microscopy and found that KLHL10 was not colocalized with either β-ACTIN or F-ACTIN (data not shown) in the seminiferous epithelium. These data suggest that KLHL10 may not be an actin-interacting protein.

PHYSIOLOGY

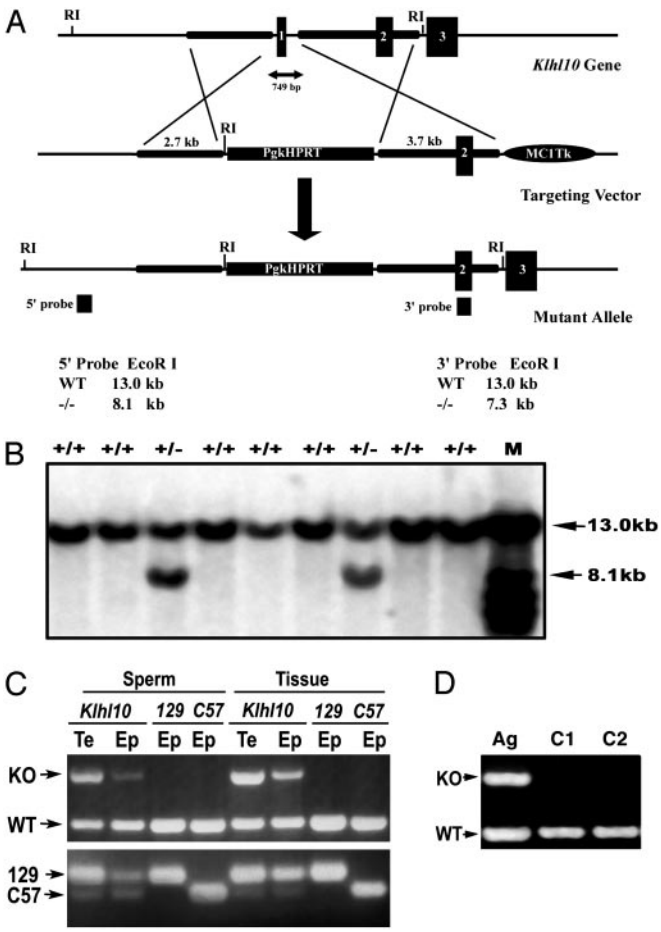

Fig. 3. Targeting of the mouse *Klhl10* in ES cells and genotyping analysis for *Klhl10* chimeric and heterozygous mutants. (*A*) *Klhl10* genomic locus and targeting vector for generation of a *Klhl10* null allele. A deletion of exon 1 (containing the start codon) of the *Klhl10* gene was achieved by homologous recombination in AB2.2 ES cells; 5′ and 3′ probes were used to distinguish WT and mutant alleles by Southern blot analysis on *Eco*RI-digested genomic DNA. (*B*) Southern blot analysis of ES cells electroporated with the targeting construct. In addition to a 13-kb WT band, a 5′ external probe detects a 8.1-kb band corresponding to the mutant allele in two ES cell clones. M, molecular weight marker. (*C*) Genotyping analyses of *Klhl10* chimeric and heterozygous males. Sperm DNA was isolated from the testis (Te) and epididymis (Ep) of a high-percentage *Klhl10* chimeric and control WT mice (129S6/SvEv and C57BL/6J strains) by using a differential digestion method (15). (*Upper*) PCR was performed to detect WT allele and knockout (KO) allele. (*Lower*) PCR was performed to detect a polymorphic locus D2Mit94, which displays a 194-bp band for the 129 strain and a 160-bp band for the C57 strain. (*D*) An agouti (Ag) male pup from a female chimera is heterozygous ($Klhl10^{+/-}$), as indicated by PCR genotyping analysis. Two WT mice were also analyzed as controls (C1 and C2).

Generation of *Klhl10* Knockout Allele. To define the physiological role of KLHL10, we generated a null allele of *Klhl10* using homologous recombination in mouse ES cells. *KLHL10* consists of five exons spanning 10–15 kb on mouse chromosome 11 or a syntenic region on human chromosome 17 (Fig. 3*A* and data not shown). We isolated a mouse genomic fragment containing *Klhl10* from a mouse genomic library (from 129S6/SvEv strain) and designed a targeting construct to generate a null *Klhl10* allele (Fig. 3*A*). The construct was electroporated into AB2.2 mouse ES cells (129S6/SvEv strain), and double selections were used to screen targeted clones as described (10). Correct targeting was verified by Southern blot analysis using both 5′ external and 3′ internal probes (Fig. 3*B*) and 21 targeted ES cell clones were obtained from 186 clones screened (11% of targeting efficiency). We injected six targeted ES cell clones and obtained 16 high-percentage chimeric (HPC) males (estimated by coat color mosaicism) and 26 low-percentage chimeric (LPC) males, as well as five LPC females.

Disrupted Spermiogenesis in HPC Males. To our surprise, 16 HPC males were completely infertile over 6 months of breeding with WT females, and 26 LPC males only produced WT C57BL/6J strain pups. We examined the genetic origin of sperm isolated from the testis and epididymis from HPC males and WT controls (129S6/SvEv and C57BL/6J) by PCR amplification of a polymorphic locus D2Mit94 (15) (Fig. 3*C Lower*). Our results indicate that >90% of testicular spermatids and total testicular cells in the HPC males originated from ES cells (129S6/SvEv strain). This finding was correlated with PCR genotypic analysis by using three primers detecting both WT and mutant alleles simultaneously (Fig. 3*C Upper*). Testicular and epididymal sperm contain the mutant allele, suggesting absence of germ-line transmission of mutant allele is not caused by absence of ES cell-derived germ cells. These findings strongly suggest that disruption of one allele of *Klhl10* results in a haploinsufficient phenotype of male infertility, similar to protamine 1 and protamine 2 knockout mice (15).

By breeding the chimeric females with WT C57BL/6J males, we obtained one heterozygous ($Klhl10^{+/-}$) male (Fig. 3*D*). This heterozygous male was also completely infertile during 6 months of breeding with WT females. Morphological and histological examinations of the testis ($Klhl10^{+/-}$) reveal abnormalities similar to the HPC males (see below and Fig. 4), confirming that disruption of spermiogenesis in those HPC males is indeed caused by haploinsufficiency of *Klhl10*.

Morphological observations revealed that the adult (8- to 24-week-old) HPC males have small testes (≈50–60% of WT), and spermiogenesis is mostly blocked in the elongating stage (after step 9) (Fig. 4*B*). In the epididymis, numerous round spermatids, elongating, and elongated spermatids are present because of sloughing of haploid germ cells into the lumen and degeneration of spermatids (data not shown). Most of the tubules are devoid of elongating and elongated spermatids. Sertoli cell vacuolization is often seen, and the severity of disruption varies from tubule to tubule. Some tubules contain only Sertoli cells, whereas some contain early germ cells and no or very few haploid cells (Fig. 4 *C* and *D*). We observed that spermatids at different maturation steps are simultaneously present in the same cross section of some tubules in young (3- to 6-week-old) and adult HPC mice, indicating asynchronized development of haploid cells during spermiogenesis (Fig. 4*F*). The asynchronized spermatid development observed during the first wave of spermatogenesis (3 weeks of age, Fig. 4*F*) suggests that the defects originate from spermatids. However, a quantitative survey by sectioning through a whole testis (5 μm thick) and counting the tubule profiles [tubules with spermatids (type A), tubules without spermatids but containing spermatocytes and spermatogonia (type B), and tubules with Sertoli cells and very few spermatogonia or only Sertoli cells (type C)] reveals every fifth section with increasing numbers of type B and type C tubules in the 24-week-old mice (10%, 50%, and 40% for type A, B, and C tubules, respectively) as compared with 8-week-old mice (60%, 35%, and 5% for type A, B, and C tubules, respectively), suggesting an enhanced disruption with the age progression in these HPC mice. The increasingly severe depletion of not only spermatids but also other germ-cell types may be caused by disruption of cellular communications due to failed spermiogenesis.

TUNEL assays revealed more apoptotic germ cells in the HPC mice than in the WT (Fig. 4). In adult WT testes, germ-cell apoptosis is a rare event (0–7 germ cells per 100 Sertoli cells) and

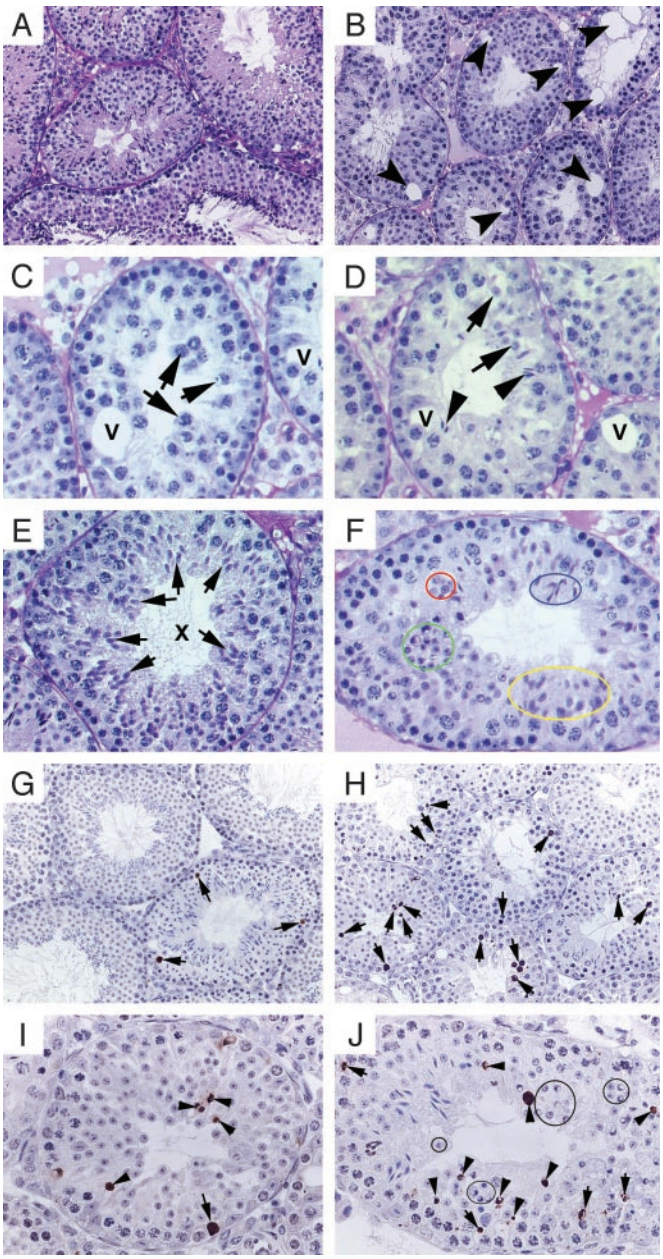

Fig. 4. Disrupted spermatogenesis in the HPC testis. *A–F* are images taken from Bouin's solution-fixed, paraffin-embedded, and periodic acid/Schiff reagent-stained testis cross sections. (*A*) Robust spermatogenesis in an 8-week-old WT mouse (×200). (*B*) A low-power image (×200) shows disrupted spermatogenesis in an 8-week-old high-percentage *Klhl10* chimeric male. Numbers of late spermatids are depleted, and multiple vacuoles (arrows) are present in the seminiferous epithelium. (*C*) A tubule from a HPC male containing spermatocytes (arrows), but no spermatids. Vacuoles (V) are present within the epithelium (×400). (*D*) A tubule from a HPC male containing fewer round spermatids (arrows) and late spermatids (arrowheads). Vacuoles (V) are present within the epithelium (×400). (*E*) A stage X tubule from a WT male displaying synchronized germ-cell maturation. All spermatids are at step 10 (arrows), which coexist with late pachytene and leptotene spermatocytes (×400). (*F*) A representative tubule with asynchronized development of haploid cells in a young (4-week-old) HPC testis (×500). Spermatids at step 5 (circled in red), steps 9–10 (yellow), and steps 11 and 12 (blue) are present simultaneously in one stage. Some spermatids appear to be degenerating (green). *G–J* are images of TUNEL assay with 4% paraformaldehyde-fixed, paraffin-embedded testis cross sections. (*G*) Three TUNEL-positive germ cells (arrows) are visible in a cross section of a WT testis (8-week-old). (*H*) Numerous TUNEL-positive germ cells (arrows) are present in a HPC testis (12-week-old). In WT testis, TUNEL-positive spermatids are rarely seen (see *G* and refs. 37 and 38). (*I*) Four TUNEL-positive round spermatids (arrowheads) and one TUNEL-positive spermatogonium (arrow) are present in this cross section of a HPC testis. (*J*) Multiple TUNEL-positive spermatids (arrowheads) and spermatocytes (arrows) are present in a cross section of a HPC (8-week-old) testis. Some morphologically apparent degenerating spermatids are TUNEL-negative (circles). (magnifications: *G* and *H*, ×200; *I* and *J*, ×400).

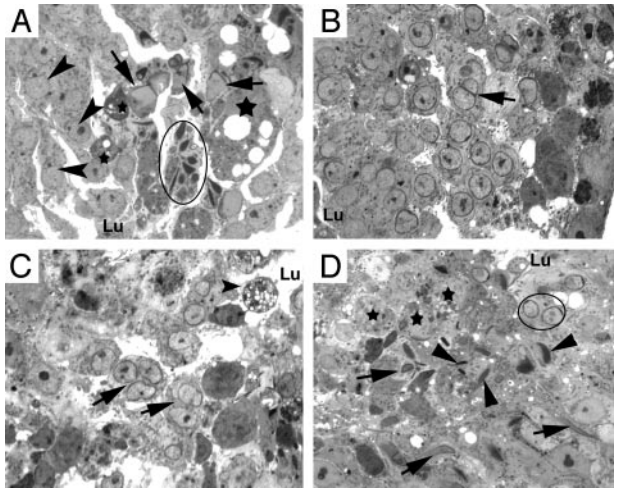

Fig. 5. High-power light microscopic analysis of spermatids in high-percentage *Klhl10* chimeric testes. (*A*) A tubule contains step 1 spermatids (arrowheads), step 9 (arrows), and steps 12 and 13 spermatids (circled). Note that multiple nuclei of step 12 and 13 spermatids appear to share a common cytoplasm, and several large or small, darkly stained, vacuolated cytoplasmic/cellular bodies (stars) are present within the epithelium. Spermatids appear to slough toward the lumen. (*B*) A tubule contains steps 8 and 9 spermatids. Two step 8 elongating spermatid nuclei (arrow) share a common acrosome and cytoplasm. (*C*) Multinucleated step 8 and 9 spermatids (arrows) are sloughing into the lumen, and large vacuolated cellular bodies are present in the seminiferous epithelium. (*D*) Disorientated and asynchronized spermatid maturation in the seminiferous epithelium. Steps 9 and 10 spermatids (arrows) coexist with step 11 and 12 spermatids (arrowheads) and step 6 and 7 round spermatids (circled). Degenerating cellular bodies (stars) are also present in the epithelium. Lu, lumen. (magnification, ×1,000).

is confined to spermatogonia, preleptotene, leptotene, zygotene, and meiotically dividing spermatocytes (at stage XII) (37, 38). In the HPC testes, in addition to apoptotic spermatogonia and spermatocytes, numerous round spermatids are also TUNEL-positive, indicating enhanced degeneration of haploid germ cells. However, some haploid spermatids that appear to be degenerating were TUNEL-negative, suggesting haploid germ cells may have an alternative degeneration pathway distinct from conventional apoptosis as suggested (39, 40).

Using semithin and high-power light microscopy, we further examined the histology of the HPC testes (Fig. 5). We observed multiple abnormalities in the haploid germ cells in the HPC testes. Most seminiferous tubules in the HPC mice are devoid of late spermatids (steps 9–16), whereas some contain few late spermatids that are often seen as multiple condensed nuclei sharing a common cytoplasm (Fig. 5*A*); some of these late spermatids have lost their proper orientation within the epithelium. Multinucleated round spermatids can be observed throughout the epithelium (Fig. 5*B*). Some step 9 spermatid nuclei share the same cytoplasm, and their acrosomes are conjoined (Fig. 5*C*). As seen in the periodic acid/Schiff-hematoxylin-stained, paraffin sections (Fig. 4), spermatids at multiple different maturation steps are present in the same cross section (Fig. 5*D*), indicating the synchronization of haploid germ-cell differentiation is disrupted. These abnormalities are reminiscent of histological changes in mice with disruption of

intercellular bridges by cytochalasin D (41) and in mice lacking *Lipe* (hormone-sensitive lipase) (42), suggesting that lowered levels of KLHL10 may cause disruptions of the integrity of the intercellular bridges (IBs) among spermatids. However, the diffuse expression pattern of KLHL10 filling the entirety of the cytoplasm of elongating and elongated spermatids does not support the possibility that KLHL10 is a component of spermatid IBs, because IB proteins should display a confined, patched expression pattern. Therefore, the asynchronized development of spermatids in our HPC mice may be secondary to other disruption due to reduced levels of KLHL10. The absence or markedly reduced number of late (elongating and elongated) spermatids coincides with the most abundant KLHL10 protein expression in *Klhl10*$^{+/-}$ and HPC males, suggesting KLHL10 has an essential role in late spermiogenesis. Disruption of one allele of *Klhl10* causes reduction of KLHL10 levels, which may affect multiple pathways that control late spermatid maturation. Because both spermatids carrying the WT allele and those having the *Klhl10*-null allele share all signaling molecules through IBs, disruptions caused by reduced levels of KLHL10 affect all late spermatid populations and result in a global failure of spermiogenesis, thus generating a haploinsufficient phenotype in *Klhl10*$^{+/-}$ and HPC males.

Several recent studies report (18–23) that at least eight BTB/Kelch proteins (structurally very similar to KLHL10) bind directly to Cullin 3 ubiquitin ligases through the BTB domain, suggesting a role of these proteins in the ubiquitination pathways. Programmed destruction of regulatory proteins through the ubiquitin-proteasome system is a widely used mechanism for controlling signaling pathways. In late spermiogenesis, transcription ceases and the ubiquitination pathway plays an important role in the regulation of protein turnover, which may be decisive to the progression of spermatid maturation (43–46). Given the high homology between those BTB-Kelch proteins and KLHL10, it is likely that KLHL10 may also be a component of the E3 ubiquitin ligase complexes, which plays an important role in the unibiquitination pathway during spermiogenesis. We should conduct yeast two-hybrid screening and coimmunoprecipitation in conjunction with MS to identify KLHL10 interacting partner(s). These experiments will give us more insight into the function of KLHL10 in spermatid development in the future. Because of haploinsufficiency, we cannot obtain a sufficient number of *Klhl10*$^{+/-}$ males for further histological examinations and molecular analyses. We are generating *Klhl10*$^{+/-}$ female mice by a conditional knockout strategy to maintain the production of *Klhl10*$^{+/-}$ males for future studies.

This work was supported in part by National Institutes of Health Specialized Cooperative Centers Program in Reproductive Research Grant HD07495 (to M.M.M.). W.Y. was supported by a postdoctoral fellowship from the Ernst Schering Research Foundation. K.H.B. is a student in the Medical Scientist Training Program at Baylor College of Medicine, supported in part by National Institutes of Health Training Grant GM07330.

1. de Kretser, D. M. & Kerr, J. B. (1993) in *The Physiology of Reproduction*, eds. Knobil, E. & Neill, J. D. (Raven, New York), Vol. 2, pp. 1177–1290.
2. Russell, L. D., Ettlin, R. A., Sinha Hikim, A. P. & Clegg, E. D. (1990) *Histological and Histopathological Evaluation of theTestis* (Cache River Press, Clearwater, FL).
3. Matzuk, M. M. & Lamb, D. J. (2002) *Nat. Cell Biol.* **4,** Suppl., s41–s49.
4. Cooke, H. J. & Saunders, P. T. (2002) *Nat. Rev. Genet* **3,** 790–801.
5. Fraccaro, M. (1983) *Differentiation (Berlin)* **23,** Suppl., S40–S43.
6. Johnson, M. D. (1998) *Fertil. Steril.* **70,** 397–411.
7. Schultz, N., Hamra, F. K. & Garbers, D. L. (2003) *Proc. Natl. Acad. Sci. USA* **100,** 12201–12206.
8. Yan, W., Rajkovic, A., Viveiros, M. M., Burns, K. H., Eppig, J. J. & Matzuk, M. M. (2002) *Mol. Endocrinol.* **16,** 1168–1184.
9. Yan, W., Ma, L., Burns, K. H. & Matzuk, M. M. (2003) *Proc. Natl. Acad. Sci. USA* **100,** 10546–10551.
10. Matzuk, M. M., Finegold, M. J., Su, J.-G. J., Hsueh, A. J. W. & Bradley, A. (1992) *Nature* **360,** 313–319.
11. Lue, Y., Rao, P. N., Sinha Hikim, A. P., Im, M., Salameh, W. A., Yen, P. H., Wang, C. & Swerdloff, R. S. (2001) *Endocrinology* **142,** 1461–1470.
12. Toppari, J. & Parvinen, M. (1985) *J. Androl.* **6,** 334–343.
13. Zhang, D., Penttila, T. L., Morris, P. L., Teichmann, M. & Roeder, R. G. (2001) *Science* **292,** 1153–1155.
14. Zhao, M., Shirley, C. R., Yu, Y. E., Mohapatra, B., Zhang, Y., Unni, E., Deng, J. M., Arango, N. A., Terry, N. H., Weil, M. M., *et al.* (2001) *Mol. Cell. Biol.* **21,** 7243–7255.
15. Cho, C., Willis, W. D., Goulding, E. H., Jung-Ha, H., Choi, Y. C., Hecht, N. B. & Eddy, E. M. (2001) *Nat. Genet* **28,** 82–86.
16. Bellve, A. R. (1993) *Methods Enzymol* **225,** 84–113.
17. Adams, J., Kelso, R. & Cooley, L. (2000) *Trends Cell Biol.* **10,** 17–24.
18. van den Heuvel, S. (2004) *Curr. Biol.* **14,** R59–R61.
19. Krek, W. (2003) *Nat. Cell Biol.* **5,** 950–951.
20. Furukawa, M., He, Y. J., Borchers, C. & Xiong, Y. (2003) *Nat. Cell Biol.* **5,** 1001–1007.
21. Geyer, R., Wee, S., Anderson, S., Yates, J. & Wolf, D. A. (2003) *Mol. Cell* **12,** 783–790.
22. Xu, L., Wei, Y., Reboul, J., Vaglio, P., Shin, T. H., Vidal, M., Elledge, S. J. & Harper, J. W. (2003) *Nature* **425,** 316–321.
23. Pintard, L., Willis, J. H., Willems, A., Johnson, J. L., Srayko, M., Kurz, T., Glaser, S., Mains, P. E., Tyers, M., Bowerman, B. & Peter, M. (2003) *Nature* **425,** 311–316.
24. Xue, F. & Cooley, L. (1993) *Cell* **72,** 681–693.
25. Ito, N., Phillips, S. E., Yadav, K. D. & Knowles, P. F. (1994) *J. Mol. Biol.* **238,** 794–814.
26. Soltysik-Espanola, M., Rogers, R. A., Jiang, S., Kim, T. A., Gaedigk, R., White, R. A., Avraham, H. & Avraham, S. (1999) *Mol. Biol. Cell* **10,** 2361–2375.
27. Robinson, D. N. & Cooley, L. (1997) *J. Cell Biol.* **138,** 799–810.
28. Hernandez, M. C., Andres-Barquin, P. J., Holt, I. & Israel, M. A. (1998) *Exp. Cell Res.* **242,** 470–477.
29. von Bulow, M., Heid, H., Hess, H. & Franke, W. W. (1995) *Exp. Cell Res.* **219,** 407–413.
30. Itoh, K., Wakabayashi, N., Katoh, Y., Ishii, T., Igarashi, K., Engel, J. D. & Yamamoto, M. (1999) *Genes Dev.* **13,** 76–86.
31. Hecht, N. B. (1998) *BioEssays* **20,** 555–561.
32. Hecht, N. B. (1988) *Prog. Clin. Biol. Res.* **267,** 291–313.
33. Hecht, N. B. (1990) *J. Reprod. Fertil.* **88,** 679–693.
34. Steger, K. (1999) *Anat. Embryol.* **199,** 471–487.
35. Steger, K. (2001) *Anat. Embryol.* **203,** 323–334.
36. Eddy, E. M. (1998) *Semin. Cell Dev. Biol.* **9,** 451–457.
37. Yan, W., Suominen, J., Samson, M., Jegou, B. & Toppari, J. (2000) *Mol. Cell. Endocrinol.* **165,** 115–129.
38. Sjoblom, T., West, A. & Lahdetie, J. (1998) *Environ. Mol. Mutagen.* **31,** 133–148.
39. Yan, W., Assadi, A. H., Wynshaw-Boris, A., Eichele, G., Matzuk, M. M. & Clark, G. D. (2003) *Proc. Natl. Acad. Sci. USA* **100,** 7189–7194.
40. Print, C. G. & Loveland, K. L. (2000) *BioEssays* **22,** 423–430.
41. Russell, L. D., Vogl, A. W. & Weber, J. E. (1987) *Am. J. Anat.* **180,** 25–40.
42. Chung, S., Wang, S. P., Pan, L., Mitchell, G., Trasler, J. & Hermo, L. (2001) *Endocrinology* **142,** 4272–4281.
43. Baarends, W. M., Roest, H. P. & Grootegoed, J. A. (1999) *Mol. Cell Endocrinol.* **151,** 5–16.
44. Baarends, W. M., van der Laan, R. & Grootegoed, J. A. (2000) *J. Endocrinol. Invest.* **23,** 597–604.
45. Grootegoed, J. A., Siep, M. & Baarends, W. M. (2000) *Baillieres Best Pract. Res. Clin. Endocrinol. Metab.* **14,** 331–343.
46. Sutovsky, P. (2003) *Microsc. Res. Tech.* **61,** 88–102.